

Low-energy $M1$ states in deformed nuclei: spin-scissors or spin-flip?

V. O. Nesterenko^{1,2,3}, P. I. Vishnevskiy^{1,4}, A. Repko⁵, J. Kvasil⁶

¹ *Laboratory of Theoretical Physics, Joint Institute for Nuclear Research, Dubna, Moscow region, 141980, Russia*

² *State University "Dubna", Dubna, Moscow Region 141980, Russia*

³ *Moscow Institute of Physics and Technology, Dolgoprudny, Moscow Region 141701, Russia**

⁴ *Institute of Nuclear Physic Almaty, Almaty Region, Kazakhstan*

⁵ *Institute of Physics, Slovak Academy of Sciences, 84511, Bratislava, Slovakia and*

⁶ *Institute of Particle and Nuclear Physics, Charles University, CZ-18000, Praha 8, Czech Republic*

The low-energy $M1$ states in deformed ^{164}Dy and spherical ^{58}Ni are explored in the framework of fully self-consistent Quasiparticle Random-Phase Approximation (QRPA) with various Skyrme forces. The main attention is paid to orbital and spin $M1$ excitations. The obtained results are compared with the prediction of the low-energy *spin-scissors* $M1$ resonance suggested within Wigner Function Moments (WFM) approach. A possible relation of this resonance to low-energy spin-flip excitations is analyzed. In connection with recent WFM studies, we consider evolution of the low-energy spin-flip states in ^{164}Dy with deformation (from the equilibrium value to the spherical limit). The effect of tensor forces is briefly discussed. It is shown that two groups of 1^+ states observed at 2.4-4 MeV in ^{164}Dy are rather explained by fragmentation of the orbital $M1$ strength than by the occurrence of the collective spin-scissors resonance. In general, our calculations do not confirm the existence of this resonance.

PACS numbers: 13.40.-f, 21.60.Jz, 27.70.+z, 27.80.+w

I. INTRODUCTION

In addition to the familiar $M1$ orbital-scissors resonance (OSR) [1–3], two specific low-energy spin-scissors resonances (SSR) were predicted within the macroscopic WFM approach, see e.g. [4–8] and references therein. While OSR is macroscopically treated as out-of-phase oscillations of proton and neutron deformed subsystems (see Fig. 1-a), two SSRs are viewed as out-of-phase oscillations of the deformed subsystems with different directions of nucleon spins. As seen from Fig. 1-b,c, the first spin-scissors resonance (SSR-1) represents oscillations of nucleons with spin-up against the nucleons with spin-down. In the second spin-scissors resonance (SSR-2), the neutron and proton spins in each scissors blade have opposite directions. So, following WFM approach, the nuclear scissors mode should have a triple structure: OSR + two SSR branches. All the scissors states should demonstrate significant $M1(K = 1)$ transitions to the ground state.

In our recent study [9], we analyzed the WFM prediction of SSR in the framework of fully self-consistent Quasiparticle Random-Phase Approximation (QRPA) method with Skyrme forces [10–13]. Our microscopic calculations have shown that particular deformed nuclei, e.g. $^{160,162,164}\text{Dy}$, can indeed exhibit at 2-3 MeV some $K^\pi = 1^+$ states with a noticeable $M1$ strength. These states are formed by ordinary spin-flip transitions between spin-orbit partners with a low orbital momentum. The states are not collective. In principle, they could be associated with the predicted SSR. However, QRPA

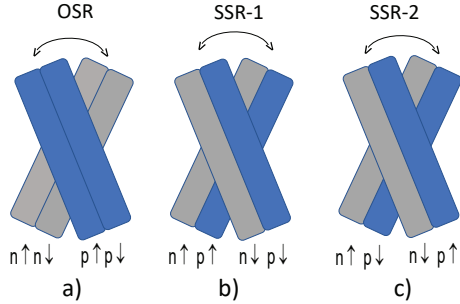


FIG. 1: Scissors triple [7]: OSR (a), SSR-1 (b), SSR-2 (c). The neutron (proton) axially deformed fractions are shown by light (dark) bars. The spin direction of nucleons is indicated by arrows. Each mode in the triple exhibits scissors-like oscillations of two blades: neutrons vs protons in OSR, spin-up vs spin-down nucleons in SSR-1 (spins of neutrons and protons in each blade have the same direction), and SSR-2 oscillations where the neutron and proton spins in each blade have opposite directions.

distributions of the nuclear current in these states do not show any signatures of the spin-scissors flow. Moreover, our calculations for $^{160,162,164}\text{Dy}$ and ^{232}Th reveal a strong interference between orbital and spin contributions to $M1$ strength. The low-energy $M1$ states turn out to be a mixture of the orbital and spin-flip modes. As a result, the experimental data in $^{160,162,164}\text{Dy}$ and ^{232}Th [14–17], treated by WFM as a confirmation of SSR, can be mainly explained by fragmentation of the orbital strength.

One of the main points disputed in QRPA [9] and WFM [8] studies is the scissors picture of the low-energy spin states. The WFM authors insist in the scissors scheme [7, 8] and WFM distributions of the nuclear cur-

*Electronic address: nester@theor.jinr.ru

rent indeed remind SSR-1 and SSR-2 modes shown in Fig. 1b,c. At the same time, in the last publications [7, 8] WFM authors accept a possible spin-flip origin of SSR. By our opinion, if we admit the spin-flip character of the low-energy of $K^\pi = 1^+$, then we should reject the scissors scheme. Indeed, the scissors excitations by definition can exist only in deformed nuclei while low-energy spin-flip states can occur in both deformed and spherical nuclei. The scissors scheme obviously contradicts the existence of low-energy spin-flip states in spherical nuclei.

To inspect this point in more detail, the evolution of low-energy $M1$ strength with decrease of the deformation parameter δ was recently studied within WFM for ^{164}Dy [8]. The obtained results look strange: the $M1$ strength, both spin and orbital, fully disappears at $\delta < 0.13 \div 0.15$. This result looks natural for the orbital $M1$ strength (which indeed has to vanish in the spherical limit) but unphysical for the spin-flip $M1$ strength (which generally has no any reason to vanish in the spherical limit).

In this connection, we suggest here investigation of low-energy $M1$ strength in ^{164}Dy in the framework of our fully self-consistent matrix QRPA method [10–13]. Various Skyrme forces (SkM* [18], SG2 [19], and two SV-forces SVbas and SV-tls [20]) are used. First of all, we inspect evolution of low-energy $M1$ strength in ^{164}Dy with decreasing nuclear quadrupole deformation. We get an expected result for the spherical limit: the orbital $M1$ strength almost vanishes while the amount of spin $M1$ strength remains almost the same. Besides, we check QRPA current distributions, including those averaged ones, but do not get the current similar to SSR-1 and SSR-2. To demonstrate the existence of low-energy spin-flip states in spherical nuclei, we calculate $M1$ strength in ^{58}Ni .

It is known that spin-flip states can be sensitive to tensor forces [21–23]. So we explore $M1$ strength in ^{164}Dy with the Skyrme parametrization SV-tls involving the tensor impact.

II. CALCULATION SCHEME

The calculations are performed within the self-consistent QRPA model [10–13] based on the Skyrme functional [24]. The model is fully self-consistent since a) both mean field and residual interaction are derived from the initial Skyrme functional b) the residual interaction takes into account all the terms following from functional, c) Coulomb (direct and exchange) parts are involved, d) both particle-hole and particle-particle channels are included [11]. The spurious admixtures caused by violation of the rotational invariance are removed using the technique [13].

The representative set of Skyrme forces is used. We employ the standard force SkM* [18], the force SG2 [19] which is widely used in the analysis of $M1$ excitations [9, 22, 25], recently developed force SVbas [20] and its analog with the tensor contribution SV-tls [20]. As seen

TABLE I: Isoscalar effective mass m_0^* , isoscalar and isovector spin-orbit parameters b_4 and b'_4 , type of pairing, and parameter β of the equilibrium axial quadrupole deformation (vs the experimental values [28]) for Skyrme forces SkM*, SG2, SVbas and SV-tls.

force	m_0^*	b_4 MeV fm ⁵	b'_4 MeV fm ⁵	pairing	β
SkM*	0.79	65.0	65.0	volume	0.354
SG2	0.79	52.5	52.5	volume	0.354
SVbas	0.90	62.32	34.11	surface	0.348
SV-tls	0.90	62.32	0.0001	surface	0.344
exper					0.349(3)

from Table I, these forces have different isoscalar b_4 and isovector b'_4 spin-orbit parameters (see their definitions in Refs. [22, 26]). In SkM* and SG2, the usual convection $b_4 = b'_4$ is used. In SVbas, the separate tuning of b_4 and b'_4 is done. The force SV-tls is constructed like SVbas but employs the full tensor spin-orbit terms. These Skyrme forces reproduce the two-hump structure of $M1(K = 1)$ spin-flip giant resonance in open-shell nuclei, see e.g. [9, 22, 25].

For axially deformed ^{164}Dy , the nuclear mean field and pairing are computed with the code SKYAX [27] using a two-dimensional grid in cylindrical coordinates. The calculation box extends up to three times the nuclear radius, the grid step is 1 fm. The axial quadrupole equilibrium deformation is obtained by minimization of the energy of the system. As seen from Table I, the obtained values of the deformation parameters β are in a good agreement with the experimental data [28], especially for SVbas. The volume and surface pairing is treated at the level of the iterative HF-BCS (Hartree-Fock plus Bardeen-Cooper-Schrieffer) method [11]. To cope with divergent character of zero-range pairing forces, energy-dependent cut-off factors are used, see for details Refs. [9, 11, 29]. The calculations for spherical ^{58}Ni are performed by a similar manner but using SKYAX version for spherical nuclei.

Both QRPA codes for deformed and spherical nuclei are implemented in the matrix form [10]. A large configuration space is used. The single-particle spectrum extends from the bottom of the potential well up to 30 MeV. For example, in SkM* calculations for ^{164}Dy , we use 693 proton and 807 neutron single-particle levels. The two-quasiparticle (2qp) basis in QRPA calculation for $K^\pi = 1^+$ states includes 4882 proton and 9702 neutron configurations.

For axially deformed nuclei, the reduced probability for $M1(K = 1)$ transitions ($M11$ in the short notation) from the ground state $|0\rangle$ to the excited QRPA state $|\nu\rangle$ with $I^\pi K = 1^+1$ reads

$$B_\nu(M11) = 2|\langle\nu|\hat{\Gamma}(M11)|0\rangle|^2. \quad (1)$$

The coefficient 2 means that contributions of both projections $K = 1$ and -1 are taken into account. The transition

operator has the form

$$\hat{\Gamma}(M11) = \mu_N \sqrt{\frac{3}{4\pi}} \sum_{qep,n} [g_s^q \hat{s}(\mu = 1) + g_l^q \hat{l}(\mu = 1)] \quad (2)$$

where μ_N is the nuclear magneton, $\hat{s}(\mu = 1)$ and $\hat{l}(\mu = 1)$ are $\mu=1$ projections of the standard spin and orbital operators, g_s^q and g_l^q are spin and orbital gyromagnetic factors. We use the quenched spin g-factors $g_s^q = \eta \bar{g}_s^q$ where $\bar{g}_s^p = 5.58$ and $\bar{g}_s^n = -3.82$ are bare proton and neutron g-factors and $\eta=0.7$ is the familiar quenching parameter [30]. The orbital g-factors are $g_l^p = 1$ and $g_l^n = 0$. In what follows, we consider three relevant cases: *spin* ($g_l^q = 0$), *orbital* ($g_s^q = 0$), and *total* (when both spin and orbital transitions are taken into account).

In deformed ^{164}Dy , the modes of multipolarities $M11$ and $E21$ are mixed. So we also calculate the reduced probability

$$B_\nu(E21) = 2|\langle \nu | \hat{\Gamma}(E21) | 0 \rangle|^2 \quad (3)$$

with the quadrupole transition operator

$$\hat{\Gamma}(E21) = e \sum_{qep,n} e_{\text{eff}}^q r^2 Y_{21}(\theta, \phi) \quad (4)$$

where $Y_{21}(\theta, \phi)$ is the spherical harmonic and e_{eff}^q are effective charges. Here we use $e_{\text{eff}}^p=1$ and $e_{\text{eff}}^n=0$. For the sake of brevity, the notations $B(M11)$ and $B(E21)$ are below replaced by the shorter notations $B(M1)$ and $B(E2)$.

We also calculate current transition densities (CTD)

$$\delta \mathbf{j}_\nu(\mathbf{r}) = \langle \nu | \hat{\mathbf{j}} | 0 \rangle(\mathbf{r}) \quad (5)$$

using operator of the convective nuclear current

$$\hat{\mathbf{j}}(\mathbf{r}) = -i \frac{e\hbar}{2m} \sum_{q=n,p} e_{\text{eff}}^q \sum_{k \in q} (\delta(\mathbf{r} - \mathbf{r}_k) \nabla_k + \nabla_k \delta(\mathbf{r} - \mathbf{r}_k)). \quad (6)$$

Here e_{eff}^q are the effective charges. They are $e_{\text{eff}}^p=1$ and $e_{\text{eff}}^n=0$ for the proton current, $e_{\text{eff}}^p=0$ and $e_{\text{eff}}^n=1$ for the neutron current, $e_{\text{eff}}^p = e_{\text{eff}}^n=1$ for isoscalar current and $e_{\text{eff}}^p = -e_{\text{eff}}^n=1$ for isovector current.

In calculation of spin-up and spin-down CTD, we project the QRPA wave function $|\nu\rangle$ to the proper spin direction using spinor structure of the involved single-particle wave functions in cylindric coordinates [31].

For ^{58}Ni , we use similar expressions relevant for spherical nuclei.

III. RESULTS AND DISCUSSION

A. ^{164}Dy : $M1$ strength and structure of 1^+ states

In Fig. 2, the total (orbital+spin) $M1$ strength at 1-4 MeV in ^{164}Dy , calculated with the forces SkM*, SG2,

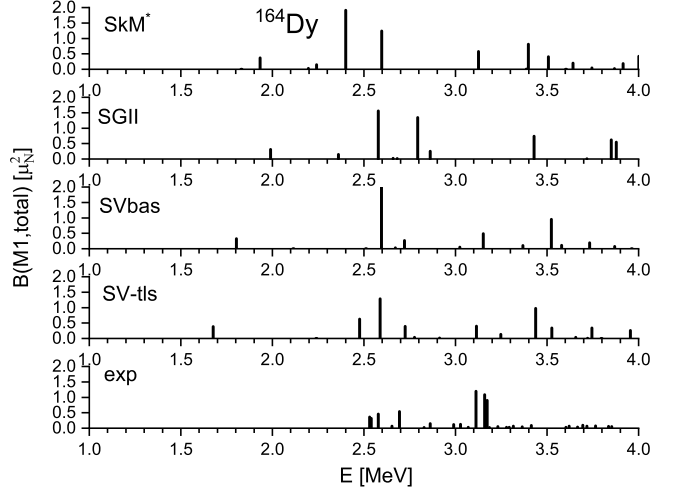


FIG. 2: Reduced transition probabilities $B(M1,\text{total})$ in ^{164}Dy , calculated with the forces SkM*, SG2, SVbas, SV-tls. QRPA results are compared with the experimental data [14].

SVbas and SV-tls, is compared with the experimental data [14]. It is seen that all four Skyrme forces give, in accordance with the experiment, a group of peaks around 2.5 MeV. The second group observed at 3.1-3.2 MeV can be roughly associated with the calculated peaks at 3.1-3.6 MeV. Below 2.4 MeV the calculations give a well separated peak located at 1.94 (SkM*), 1.98 (SG2), 1.81 (SVbas) and 1.68 (SV-tls) MeV. As shown below, this peak has a spin-flip origin. Note that database [28] suggests a tentative 1^+ state at 1.74 MeV. The comparison of SVbas and SV-tls results shows that impact of tensor forces on low-energy 1^+ states in ^{164}Dy is rather weak.

In Table II, we demonstrate features of some relevant 1^+ states in ^{164}Dy , calculated with different Skyrme forces. For all the forces, the lowest 1^+ state is dominated by two-quasiparticle (2qp) proton configuration $pp[411 \uparrow, 411 \downarrow]$ and so is basically of a spin-flip character. In this state, we obtain $B(M1, \text{spin}) > B(M1, \text{orbit})$. For SkM* and SG2, the second 1^+ state is also spin-flip one but now with the dominant neutron component $nn[521 \uparrow, 521 \downarrow]$. The origin of these proton and neutron 2qp spin-flip components in Dy isotopes is discussed in detail in our previous study [9]. Other states in Table II are basically orbital with $B(M1, \text{orbit}) > B(M1, \text{spin})$. These states are more collective than spin-flip ones. The column "F-pos" shows that all the considered excitations are formed by particle-hole (1ph) transitions.

It is easy to see that in most of the considered states there is a significant interference of the spin and orbital contributions in the total $M1$ transition. In other words, $B(M1, \text{spin}) + B(M1, \text{orbit}) \neq B(M1, \text{total})$. The interference is usually destructive in spin-flip states and constructive in orbital states. So, in all the states, the spin and orbital $M1$ modes are mixed. WFM also predicts a mixture of OSR, SSR-1 and SSR-2 [7, 8].

TABLE II: Characteristics of particular low-energy $K^\pi = 1^+$ states in ^{164}Dy , calculated within QRPA with the forces SkM*, SG2, SVbas and SV-tls. For each state, we show the excitation energy E , orbital, spin and total reduced transition probabilities $B(M1)$ and main 2qp components (contribution to the state norm in %, structure in terms of Nilsson asymptotic quantum numbers, position of the involved single-particle states relative to the Fermi level F).

force	E	$B(M1)[\mu_N^2]$			Main 2qp components		
		[MeV]	orb	spin	total	%	[N, n_z, Λ]
SkM*	1.93	0.03	0.37	0.18	96	$pp[411 \uparrow, 411 \downarrow]$	F-1, F+1
					2	$nn[521 \uparrow, 521 \downarrow]$	F-2, F+1
	2.24	≈ 0	0.11	0.07	80	$nn[521 \uparrow, 521 \downarrow]$	F-2, F+1
					17	$nn[521 \uparrow, 523 \uparrow]$	F-2, F
SG2	2.40	0.53	0.06	0.96	71	$nn[642 \uparrow, 633 \uparrow]$	F-1, F+2
					16	$pp[532 \uparrow, 523 \uparrow]$	F-2, F+2
	2.60	0.25	0.08	0.62	56	$pp[532 \uparrow, 523 \uparrow]$	F-2, F+2
					13	$nn[521 \uparrow, 512 \uparrow]$	F-2, F+3
SVbas	1.99	0.01	0.25	0.15	99	$pp[411 \uparrow, 411 \downarrow]$	F, F+1
	2.36	≈ 0	0.09	0.07	98	$nn[521 \uparrow, 521 \downarrow]$	F-2, F+1
	2.58	0.42	0.05	0.78	73	$nn[642 \uparrow, 633 \uparrow]$	F, F+2
					11	$pp[532 \uparrow, 523 \uparrow]$	F-1, F+2
SV-tls	2.79	0.31	0.07	0.67	62	$pp[532 \uparrow, 523 \uparrow]$	F-1, F+2
					12	$nn[521 \uparrow, 512 \uparrow]$	F-2, F+3
	1.80	0.03	0.32	0.16	99	$pp[411 \uparrow, 411 \downarrow]$	F, F+1
	2.59	0.41	0.14	1.02	69	$pp[532 \uparrow, 523 \uparrow]$	F-1, F+2
					8	$nn[521 \uparrow, 521 \downarrow]$	F-2, F+1
	2.72	0.10	≈ 0	0.13	71	$nn[642 \uparrow, 633 \uparrow]$	F-1, F+2
					13	$nn[521 \uparrow, 512 \uparrow]$	F-2, F+3
	1.67	0.07	0.50	0.19	95	$pp[411 \uparrow, 411 \downarrow]$	F, F+1
					2	$nn[521 \uparrow, 521 \downarrow]$	F-3, F+1
	2.48	0.17	0.02	0.31	52	$pp[532 \uparrow, 523 \uparrow]$	F-1, F+2
					25	$nn[521 \uparrow, 521 \downarrow]$	F-3, F+1
	2.59	0.18	0.15	0.64	67	$nn[521 \uparrow, 521 \downarrow]$	F-3, F+1
					23	$pp[532 \uparrow, 523 \uparrow]$	F-1, F+2

B. ^{164}Dy : current fields

It is instructive to consider distributions of the nuclear current in 1^+ states. In Fig. 3, we show average distributions of the proton, neutron, isoscalar ($\Delta T=0$) and isovector ($\Delta T=1$) convective CTD in ^{164}Dy . Here we average CTD for all QRPA states at 2.25 - 4 MeV, i.e. at the energy range where most of the orbital $M1$ strength is concentrated. The averaging allows to smooth individual peculiarities of the currents of particular QRPA states and thus highlight the main common features of the nuclear current in the chosen energy range. The procedure of averaging is described in Ref. [32].

In Fig. 3, the proton current reminds a motion of a fluid contained in the rotating ellipsoidal vessel [33, 34]. In this picture, the local flows at the poles and left/right sides have opposite directions. In our case, the side flows

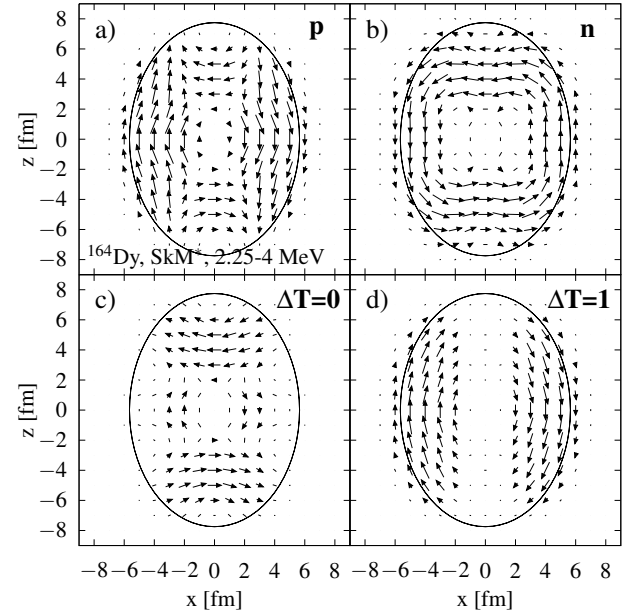


FIG. 3: QRPA SkM* proton (a), neutron (b), isoscalar (c) and isovector (d) distributions of the nuclear current (convective CTD on (x,z) plane), averaged at the energy range 2.25-4 MeV in ^{164}Dy . The solid ellipse shows the nuclear boundary.

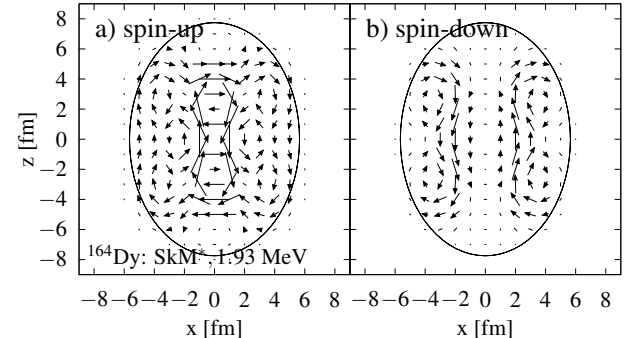


FIG. 4: SkM* spin-up (a) and spin-down (b) CTD for the lowest QRPA 1^+ state at 1.93 MeV in ^{164}Dy . The solid ellipse shows the nuclear boundary.

are clockwise and pole flows are anticlockwise. Instead, in the neutron current, both pole and side flows are anticlockwise. The general flow is mainly isoscalar (IS) on the poles and isovector (IV) on the sides. In principle, the IV side flows can be associated with OSR, though this somewhat contradicts OSR scheme where the most strong flow is expected in the pole regions.

Figure 4 shows spin-up and spin-down currents for the lowest SkM* 2qp spin-flip state at 1.93 MeV. Both currents have a complicated structure and do not match smooth SSR-1 currents exhibited in Refs. [7, 8]. Perhaps, the difference is partly caused by the fact that, unlike the collective SSR-1 states, QRPA suggests almost 2qp spin-flip states whose currents are not smooth.

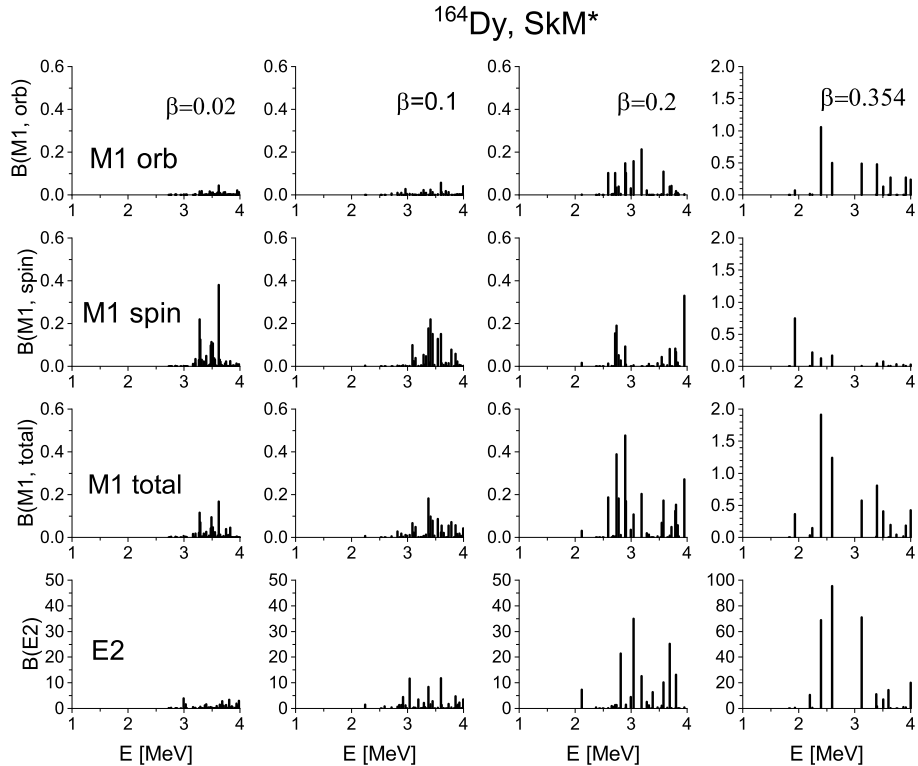


FIG. 5: Reduced transition probabilities $B(M1, \text{orb})$, $B(M1, \text{spin})$, $B(M1, \text{total})$ (in μ_N^2) and $B(E2)$ (in $e^2 \text{ fm}^4$) in ^{164}Dy , calculated with the force SkM* for different quadrupole deformations $\beta=0.02, 0.1, 0.2, 0.354$.

C. ^{164}Dy : spherical limit

The most disputed point in WFM results is the spin-scissors treatment of low-energy 1^+ states, which can be actually realized only in deformed nuclei. At the same time, spin-flip states can exist in both deformed and spherical nuclei. In this connection it is worth to inspect the spherical limit for low-energy 1^+ states. Such WFM analysis was recently performed for ^{164}Dy [8]. It was shown that for all three scissors modes (OSR, SSR-1 and SSR-2) the $M1$ strength fully disappears at the deformation $\delta=0.135-0.165$ ($\delta = 0.95\beta$). This result looks doubtful since, if we accept spin-flip character of SSR-1 and SSR-2, then their $M1$ strength should not fully vanish in the spherical limit.

This point is inspected in Fig. 5, where we show SkM* QRPA $M1$ strengths in ^{164}Dy , calculated at $\beta=0.02, 0.1, 0.2$ and 0.354 (the last value is SkM* equilibrium deformation). We see that, as expected, the low-energy orbital strength $B(M1, \text{orbit})$ significantly decreases at $\beta \rightarrow 0$. The quadrupole strength $B(E2)$ exhibited at the lower panels follow the same trend. Instead, spin strength $B(M1, \text{spin})$ is downshifted by energy and *increases* its integral value. The later is in drastic contradiction with WFM result [8]. In accordance with Table II, Fig. 5 shows a strong interference of the orbital and spin contributions to $M1$ strength.

The above trends for $M1$ and $E2$ strengths become

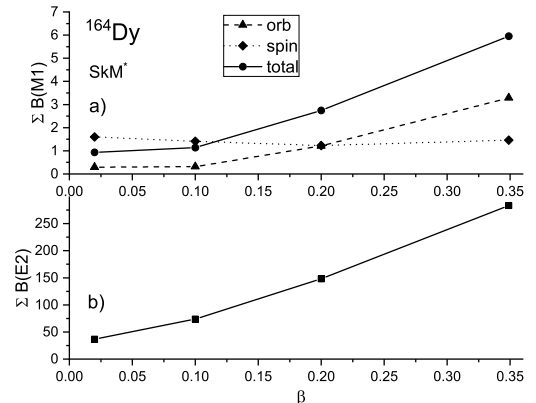


FIG. 6: a) Orbital (red triangles connected by dashed line), spin (blue rhombuses connected by dotted line) and total (black circles connected by solid line) summed $B(M1)$ values calculated with the force SkM* for $\beta=0.02, 0.1, 0.2$ and 0.354 . b) The summed $B(E2)$ values for the same deformations.

even more apparent in Fig. 6 where these strengths are summed at 0-4 MeV. We see that the total $M1$ strength is dominated by the spin contribution at $\beta < 0.2$ and by orbital contribution at a higher deformation. The orbital $M1$ and quadrupole $E2$ strengths vanish at $\beta \rightarrow 0$ while the spin $M1$ strength even somewhat increases.

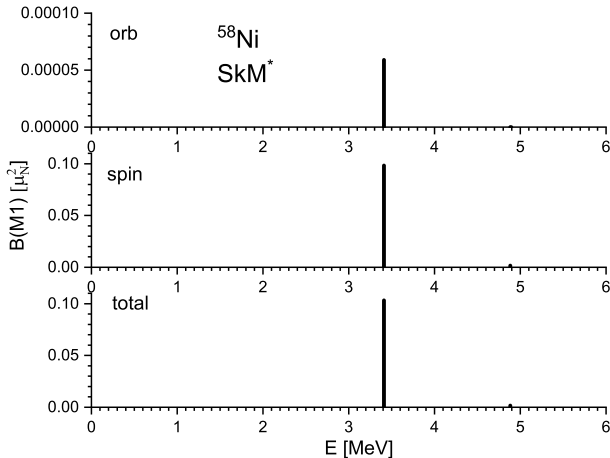


FIG. 7: Reduced transition probabilities $B(M1)$ in ^{58}Ni for the orbital, spin and total cases, calculated with the force SkM^* . Note the different scale for the orbital case.

D. ^{58}Ni

As mentioned above, low-energy spin-flip $M1$ states should exist in both deformed and spherical nuclei. The latter is demonstrated in Fig. 7 where orbital, spin and total $B(M1)$ values are exhibited for the states at 0-6 MeV in spherical ^{58}Ni . Actually, in this energy range, only the lowest $I^\pi = 1^+$ state at 3.41 MeV is visible (the next state at 4.9 MeV exhibits very small $M1$ strength and so is almost invisible in the figure). The lowest state is almost fully (99.5%) exhausted by 2qp spin-flip neutron configuration $nn[2p_{3/2}, 2p_{1/2}]$ and so is the pure spin-flip excitation. This example shows that, in contradiction with the WFM conclusion [8], low-energy spin-flip states *can* exist in spherical nuclei. This can take place under some obvious conditions: the spin-flip transition should be of 1ph-character and connect spin-orbit partners with a low orbital moment. Both these conditions are fulfilled in ^{58}Ni .

Note that other Skyrme forces give similar energies for the lowest spin-flip $I^\pi = 1^+$ state in ^{58}Ni , e.g. 3.42 MeV (SG2) and 3.02 MeV (SVbas). These values are in a good agreement with the experimental energy 2.902 MeV of the lowest 1^+ state in ^{58}Ni [28].

Acknowledgements

The authors thank Prof P.-G. Reinhard for the code SKYAX. A.R. acknowledges support by the Slovak Research and Development Agency under Contract No. APVV-20-0532 and by the Slovak grant agency VEGA (Contract No. 2/0067/21). J.K. appreciates the support by a grant of the Czech Science Agency, Project No. 19-14048S.

IV. CONCLUSIONS

The prediction of the Wigner Function Moment (WFM) method on existence of low-energy spin-scissors resonances (SSR) in deformed nuclei [4-8] was analyzed in the framework of the self-consistent Quasiparticle Random-Phase Approximation (QRPA) approach. The representative set of Skyrme forces (SkM^* , SG2, SVbas, and SV-tls) was applied. The main analysis was done for deformed ^{164}Dy which, following WFM predictions, is one of the best candidates for the search of SSR.

Our calculations show that the lowest $K^\pi = 1^+$ states in ^{164}Dy have a spin-flip character. These states lie at 1.5-2.4 MeV and represent almost pure two-quasiparticle (2qp) excitations. In principle, these states could be roughly associated with the predicted SSR. However, there are some arguments against such association. First, unlike WFM prediction, these states are not collective. Second, their current distributions significantly differ from WFM SSR currents. Perhaps, the latter is caused by 2qp character of the lowest spin-flip states, which makes the current distribution complicated and state-dependent.

In our SkM^* calculations, a part of the orbital strength is downshifted to the SSR region ($E \leq 2.25$ MeV) and, vice versa, the OSR region hosts some spin-flip strength. As a result, even at the energy range $2.25 \text{ MeV} < E < 4$ MeV, where $M1$ strength is mainly orbital, 1^+ states demonstrate a significant interference of the major orbital and minor spin-flip components.

The experimental data [14] show two distinctive low-energy groups of 1^+ states in ^{164}Dy . They are located at 2.5-2.7 MeV and 3.1-3.2 MeV, respectively. These two groups are treated by WFM as SSR and OSR. However, in our calculations, spin-flip states lie at $E \leq 2.4$ MeV, i.e. below the first observed group. Moreover, following our results, both groups of the observed 1^+ states are mainly produced by fragmentation of the orbital strength. So, perhaps these experimental data cannot be considered as the SSR evidence.

The WFM *scissors-like* treatment of SSR assumes the nuclear deformation. Following WFM study [8], $M1$ strength fully vanishes already at the deformations $\delta=0.135-0.165$. So it is concluded that SSR cannot exist in spherical nuclei. Instead, our QRPA calculations for ^{164}Dy show that spin-flip $M1$ strength remains strong even in the spherical limit. Moreover, we show that the lowest $I^\pi = 1^+$ state at 3.4 MeV spherical ^{58}Ni is spin-flip one. So, in contradiction with WFM conclusions, low-energy $M1$ states of the spin character *can* exist in spherical nuclei.

Altogether, one may conclude that our present QRPA calculations do not confirm the existence of SSR. Perhaps, more studies are necessary to draw the final conclusions. It would be useful to include to the self-consistent microscopic analysis the coupling with complex configurations. As for WFM, the strange result with disappearance of $M1$ strength in the spherical limit should

be checked. Besides, to our knowledge, the giant spin-flip $M1$ resonance does not appear in WFM calculations, which make questionable any analysis of spin modes within this model. Further, WFM calculations give in ^{164}Dy the 1.47-MeV $K^\pi = 1^+$ state with a huge $B(E2)$ value [7]. Such state is absent in both experiment and

numerous microscopic calculations.

Finally note that low-energy spin-flip $M1$ states can be sensitive to tensor forces. In our calculations for ^{164}Dy , the effect of tensor force is modest. Anyway, low-energy spin-flip $M1$ states are in general very promising object for investigation of the impact of tensor forces.

-
- [1] N. Lo Iudice and F. Palumbo, Phys. Rev. Lett. **41**, 1532 (1978).
- [2] D. Bohle, A. Richter, W. Steffen, A.E.L. Dieperink, N. Lo Iudice, F. Palumbo, and O. Scholten, Phys. Lett. B **137**, 27 (1984).
- [3] N. Lo Iudice, Part. Nucl. **28**, n.6, 1389 (1997).
- [4] E.B. Balbutsev, I.V. Molodtsova, and P. Schuck, Nucl. Phys. A **872**, 42 (2011).
- [5] E.B. Balbutsev, I.V. Molodtsova, and P. Schuck, Phys. Rev. C **91**, 064312 (2015).
- [6] E.B. Balbutsev, I.V. Molodtsova, and P. Schuck, Phys. Rev. C **97**, 044316 (2018).
- [7] E.B. Balbutsev, I.V. Molodtsova, A.V. Sushkov, N.Yu. Shirikova and P. Schuck, Phys. Rev. C **105**, 044323 (2022).
- [8] E.B. Balbutsev, Phys. Atom. Nucl. **85**, 338 (2022).
- [9] V.O. Nesterenko, V.I. Vishnevskiy, J. Kvasil, A. Repko and W. Kleinig, Phys. Rev. C **103**, 064313 (2021).
- [10] A. Repko, J. Kvasil, V.O. Nesterenko, P. G. Reinhard, arXiv:1510.01248 (nucl-th), 2015.
- [11] A. Repko, J. Kvasil, V.O. Nesterenko, P.-G. Reinhard, Eur. Phys. J. A **53**, 221 (2017).
- [12] A. Repko, J. Kvasil, and V.O. Nesterenko, Phys. Rev. C **99**, 044307 (2019).
- [13] J. Kvasil, A. Repko, and V.O. Nesterenko, Eur. Phys. J. A **55**, 213 (2019).
- [14] J. Margraf, T. Eckert, M. Rittner, I. Bauske, O. Beck, U. Kneissl, H. Maser, H. H. Pitz, A. Schiller, P. von Brentano, R. Fischer, R.-D. Herzberg, N. Pietralla, A. Zilges, and H. Friedrichs, Phys. Rev. C **52**, 2429 (1995).
- [15] S. Valenta, B. Baramsai, T.A. Bredeweg, A. Couture, A. Chyzh, M. Jandel, J. Kroll, M. Krtička, G. E. Mitchell, J.M. O'Donnell, G. Rusev, J.L. Ullmann, and C. L. Walker, Phys. Rev. C **96**, 054315 (2017).
- [16] T. Renstrøm, H. Utsunomiya, H.T. Nyhus, A.C. Larsen, M. Guttormsen, G.M. Tveten, D.M. Filipescu, I. Gheorghie, S. Goriely, S. Hilaire, Y.-W. Lui, J.E. Midtbø, S. Pérus, T. Shima, S. Siem, and O. Tesileanu, Phys. Rev. C **98**, 054310 (2018).
- [17] A.S. Adekola, C.T. Angell, S.L. Hammond, A. Hill, C.R. Howell, H.J. Karwowski, J.H. Kelley, and E. Kwan, Phys. Rev. C **83**, 034615 (2011).
- [18] J. Bartel, P. Quentin, M. Brack, C. Guet, and H.-B. Håkansson, Nucl. Phys. A **386**, 79 (1982).
- [19] N. Van Giai and H. Sagawa, Phys. Lett. B **106**, 379 (1981).
- [20] P. Klüpfel, P.-G. Reinhard, T.J. Bürvenich, and J.A. Maruhn, Phys. Rev. C **79**, 034310 (2009).
- [21] G. Colò, H. Sagawa, S. Fracasso and P.F. Bortignon, Phys. Lett. B **646**, 227 (2007).
- [22] P. Vesely, J. Kvasil, V.O. Nesterenko, W. Kleinig, P.-G. Reinhard, and V.Yu. Ponomarev, Phys. Rev. C **80**, 031302(R) (2009).
- [23] Shihang Shen, Haozhao Liang, Jie Meng, Peter Ring, and Shuangquan Zhang, Phys. Lett. B **778**, 344 (2018).
- [24] M. Bender, P.-H. Heenen, and P.-G. Reinhard, Rev. Mod. Phys. **75**, 121 (2003).
- [25] V.O. Nesterenko, J. Kvasil, P. Vesely, W. Kleinig, P.-G. Reinhard, and V.Yu. Ponomarev, J. Phys. G: Nucl. Part. Phys. **37**, 064034 (2010).
- [26] J. R. Stone and P.-G. Reinhard, Prog. Part. Nucl. Phys. **58**, 587 (2007).
- [27] P.-G. Reinhard, B. Schuetrumpf, and J.A. Maruhn, Comput. Phys. Commun. **258**, 107603 (2021).
- [28] Database <http://www.nndc.bnl.gov>.
- [29] M. Bender, K. Rutz, P.-G. Reinhard, and J.A. Maruhn, Eur. Phys. J. A **8**, 59 (2000).
- [30] M. N. Harakeh and A. van der Woude, *Giant Resonances* (Clarendon Press, Oxford, 2001).
- [31] V.O. Nesterenko, W. Kleinig, J. Kvasil, P. Vesely, P.-G. Reinhard, and D.S. Dolci, Phys. Rev. C **74**, 064306 (2006).
- [32] A. Repko, P.-G. Reinhard, V.O. Nesterenko, and J. Kvasil, Phys. Rev. C **87**, 024305 (2013).
- [33] A. Bohr and B. R. Mottelson, *Nuclear Structure, Vol. II* (World Scientific, Singapore, 1998).
- [34] I.N. Mikhailov, Ch. Briançon and P. Quentin, Part. Nucl. **27**, n.2, 303 (1996).